Kobe University Repository : Kernel

PDF issue: 2025-08-08

Rapid-scan broadband frequency-domain terahertz spectroscopy via dynamic optical phase lock

Shoji, Yuto
Ohmichi, Eiji
Takahashi, Hideyuki
Ohta, Hitoshi

(Citation)
Applied Physics Letters,125(3):031102

(Issue Date)
2024-07-15

(Resource Type)
journal article

(Version)
Version of Record

(Rights)
© 2024 Author(s). Published under an exclusive license by AIP Publishing. This article may be downloaded for personal use only. Any other use requires prior permission of the author and AIP Publishing. This article appeared in Appl. Phys. Lett. 125, 031102 (2024) and may be found at at https://doi.org/10.1063/5.0215826

(URL)
https://hdl.handle.net/20.500.14094/0100491424

KOBE UNIVERSITY

Applied Physics Letters

RESEARCH ARTICLE | JULY 15 2024

Rapid-scan broadband frequency-domain terahertz spectroscopy via dynamic optical phase lock

Yuto Shoji ; Eiji Ohmichi ; Hideyuki Takahashi ; Hitoshi Ohta

Check for updates

Appl. Phys. Lett. 125, 031102 (2024)
https://doi.org/10.1063/5.0215826

View Online
Export Citation

15 July 2024 23:25:19

AIP Publishing

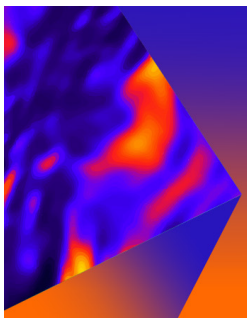

Applied Physics Letters

Special Topic: Mid and Long Wavelength Infrared Photonics, Materials, and Devices

Submit Today

AIP Publishing

Applied Physics Letters ARTICLE pubs.aip.org/aip/apl

Rapid-scan broadband frequency-domain terahertz spectroscopy via dynamic optical phase lock

Cite as: Appl. Phys. Lett. **125**, 031102 (2024); doi: 10.1063/5.0215826
Submitted: 26 April 2024 · Accepted: 29 June 2024 ·
Published Online: 15 July 2024

View Online Export Citation CrossMark

Yuto Shoji,[1] Eiji Ohmichi,[1,a)] Hideyuki Takahashi,[2] and Hitoshi Ohta[1,2]

AFFILIATIONS

[1]Graduate School of Science, Kobe University, 1-1 Rokkodai, Nada, Kobe 657-8501, Japan
[2]Molecular Photoscience Research Center, Kobe University, 1-1 Rokkodai, Nada, Kobe 657-8501, Japan

[a)]Author to whom correspondence should be addressed: ohmichi@harbor.kobe-u.ac.jp

ABSTRACT

Frequency-domain terahertz (THz) spectroscopy using photomixing devices has unique advantages such as high dynamic range and high spectral resolution. Thus, many applications for solid-state and gas-phase spectroscopy have been proposed. In this study, we developed a feedback controlled technique to dynamically compensate for the optical phase accompanied by frequency sweep, enabling both fast and high-resolution data acquisition across a wide frequency region. From gas-phase THz spectroscopy measurements of dilute acetonitrile gas in a wide frequency range up to 1.1 THz, fine structures with linewidths less than 10 MHz were clearly resolved, while the data acquisition rate was improved by two orders compared to the previously reported value.

Published under an exclusive license by AIP Publishing. https://doi.org/10.1063/5.0215826

15 July 2024 23:25:19

Terahertz (THz) spectroscopy has gained much attention in recent years due to its wide range of applications, including nondestructive inspection,[1] process control,[2,3] and imaging.[4,5] For decades, various types of THz generation/detection techniques have been developed. Among them, the most widely prevailing technique is time-domain THz spectroscopy,[6] in which THz pulses are emitted from either ultrafast photoconductive switches or nonlinear optical crystals.[7–10] This technique provides unique opportunities for THz spectroscopy featuring fast data acquisition rates across a wide frequency range of up to 6.5 THz,[11–13] though its spectral resolution is limited to at most 0.6 GHz. On the other hand, frequency-domain THz spectroscopy,[14–19] in which photomixing devices are used for continuous-wave and tunable THz generation/detection, has the advantages of a relatively wide bandwidth of up to 4.5 THz[20] and a high spectral resolution of the order of 1 MHz.[21,22] Indeed, our group has applied such a high-resolution spectroscopy technique to terahertz electron paramagnetic resonance (EPR) spectroscopy,[23,24] where a sharp EPR signal with a linewidth of 20 MHz is clearly observed.[21,25]

In the previous frequency-domain THz spectrometers,[21,25,26] a pair of fiber stretchers was used to measure the amplitude of THz waves at each frequency, and the frequency was swept step by step to cover the desired frequency range. However, it inevitably takes a rather long acquisition time (typically several seconds per data point) for the fiber stretchers to execute phase sweeps. This drawback practically hinders broadband measurements of high-resolution THz spectroscopy. To solve this problem, we developed a feedback-controlled technique to measure the THz wave amplitude instantaneously by utilizing dynamic phase lock. This allowed us to achieve a faster data acquisition rate by about two orders, enabling broadband and high-resolution THz spectroscopy. In this Letter, real-time gas-phase spectroscopy of dilute acetonitrile was also demonstrated as a promising application of the present work.

For the continuous generation of THz waves via photomixing, two single-mode laser beams with slightly different frequencies are coupled and irradiated onto a voltage-biased photoconductive antenna (PCA) of an emitter. By adjusting the mutual frequency difference in the THz range, coherent THz waves are emitted from the emitter antenna through a hemispherical Si lens.[27] The emitted THz waves are detected by a receiver antenna using a homodyne technique.[28,29]

The THz wave amplitude and the measured photocurrent (I_{ph}) flowing in the receiver antenna are related by the following equation:

$$I_{\mathrm{ph}} \propto E_{\mathrm{THz}} \cos(2\pi \Delta L f_{\mathrm{THz}}/c) = E_{\mathrm{THz}} \cos(\Delta\varphi), \quad (1)$$

where E_{THz} is the electric field component of THz waves, c is the speed of light, ΔL is the optical path difference between the emitter and receiver branches, f_{THz} is the THz frequency, and $\Delta\varphi$ is the optical

Published under an exclusive license by AIP Publishing

phase difference. This equation indicates that the photocurrent oscillates when f_{THz} is swept, and it is necessary to determine the envelope E_{THz} as a function of f_{THz}. These oscillations stem from the optical interference between the emitter and receiver branches. Typically, its oscillation frequency $c/\Delta L$ ranges on the order of several GHz, depending on the initial path difference ΔL. Therefore, the frequency resolution for the case of envelope detection is inevitably limited by this oscillatory behavior of I_{ph}.

In our previous report,[21,25] the optical phase was widely swept at a fixed frequency using a fiber stretcher ($\Delta L \rightarrow \Delta L + \delta L$) so that the induced optical phase difference $2\pi\delta L f_{\mathrm{THz}}/c$ exceeded 2π. Then, E_{THz} was unambiguously obtained by the oscillation amplitude of I_{ph} at each frequency. However, the phase sweep/readout and subsequent frequency-step processes took more time than simply sweeping the THz frequency. We therefore developed a feedback-controlled technique to improve the data acquisition rate, in which I_{ph} always stays at its extremal values by instantaneously adjusting the optical phase difference to $\Delta\varphi = n\pi$ (n : integer).

Figure 1(a) illustrates the setup of our frequency-domain THz spectrometer developed in this study. We used commercially available InGaAs photomixers (TeraScan1550, TOPTICA) for broadband emission and detection of THz waves from 50 to 1100 GHz. The emitted THz waves were linearly polarized, since bow-tie antennas were incorporated in the photomixers. The nominal power was 100 and 10 μW at 100 and 500 GHz, respectively, according to the manufacture's specification. THz waves emitted from the PCA emitter pass through a gas cell and are detected by the PCA receiver using a homodyne technique. A pair of plastic lenses was used to collimate and refocus the THz waves. Sinusoidal bias voltages ($f = 40$ kHz) were applied to the PCA emitter, and the resulting synchronous components of the receiver photocurrent, followed by an I/V converter, were detected by an FPGA-based lock-in amplifier (LIA1) installed in the hardware of TeraScan1550 and an external lock-in amplifier (LIA2). The initial optical path difference was not optimized to a specific value and was typically $\Delta L = 0.1$ m in this study.

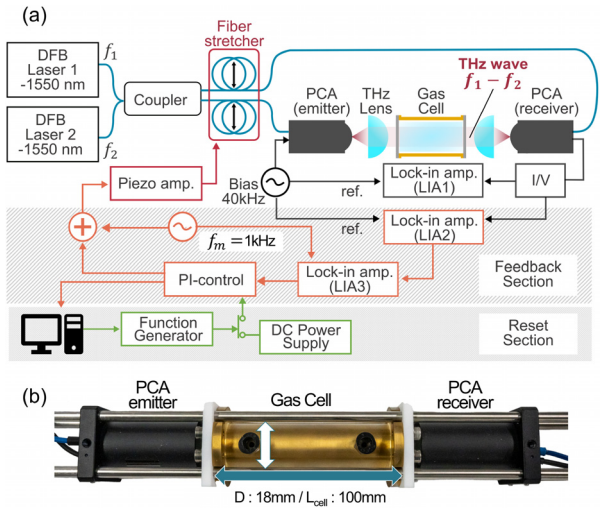

FIG. 1. (a) Experimental setup of our frequency-domain THz spectrometer using continuously tunable PCA photomixers. The system consists of the THz optics part, the feedback part, and the reset part. (b) Photograph of the THz optics part including a PCA emitter, a gas cell, and a PCA receiver.

Small sinusoidal voltages were applied to the fiber stretcher to modulate the optical phase difference. Typically, the amplitude and frequency were a few volts and $f_{\mathrm{m}} = 1$ kHz, respectively. This phase modulation induced the photocurrent modulation. We set the time constants of LIA1 (τ_1) and LIA2 (τ_2) to satisfy the condition $1/f < \tau_2 < 1/f_{\mathrm{m}} < \tau_1$. As a result, the fundamental component of the output of LIA2 was modulated at f_{m}, but that of LIA1 was averaged out. The signal-to-noise (SNR) ratio of our spectrometer was typically 60 dB at 500 GHz with $\tau_1 = 30$ ms.

When the optical phase difference is modulated as $\Delta\varphi = \Delta\varphi_0 + \delta\varphi \sin(\omega_{\mathrm{m}} t)$ using the fiber stretchers, a series expansion of Eq. (1) leads to $I_{\mathrm{ph}} \propto J_0(\delta\varphi)\cos(\Delta\varphi_0) + 2\sum_{n=2,\mathrm{even}}^{\infty} J_n(\delta\varphi)\cos(\Delta\varphi_0) \times \cos(n\omega_m t) + 2\sum_{n=1,\mathrm{odd}}^{\infty} J_n(\delta\varphi)\sin(\Delta\varphi_0)\sin(n\omega_m t)$, where J_n is the nth order Bessel function, $\Delta\varphi_0$ is the initial optical phase difference, $\delta\varphi$ is the modulation amplitude of the optical phase, and $\omega_m = 2\pi f_m$. This equation indicates that I_{ph} contains both the fundamental and higher harmonic terms in general, but at the extrema of I_{ph} where $\Delta\varphi_0 = n\pi$ holds, the odd terms become zero. Therefore, if $\Delta\varphi_0$ is adjusted such that the fundamental component ($n = 1$) of the output of LIA2 becomes zero, I_{ph} always remains at its extrema.

This is the basic principle to continuously obtain the photocurrent amplitude during a frequency sweep. For this purpose, a feedback system was used to add proper dc bias voltages to the fiber stretchers. This is done by a combination of another lock-in amplifier (LIA3) and a home-built PI-control circuit. LIA3 demodulates the component at f_m, and its amplitude is fed into the control circuit to produce negative-feedback signals. As a result, the optical phase difference was locked to keep the I_{ph} value at its extrema. It was confirmed that the data measured by LIA1 entirely coincided with the envelope of I_{ph} measured without the feedback circuit (see the supplementary material).

In our system, the reset circuit was incorporated to extend the frequency range. Consider the case where frequency is swept in the range of $f_{\mathrm{THz}} = 0.1$–1.1 THz with an initial optical path difference of $\Delta L = 0.1$ m, the total optical phase difference exceeds 300π. Such a large phase difference cannot be compensated by a single voltage sweep of the fiber stretcher. Indeed, the voltage-induced phase shift was at most 5 π at 500 GHz, thus being impossible to add a proper optical phase difference in a single operation. So, the reset section was programmed to switch off the feedback circuit once to reset and to initialize the circuit when the output voltages reached its maximum voltage. During this operation, a short interruption time of about 100 ms was needed, but it did not influence the total measurement time.

In the following, this technique was applied to gas-phase spectroscopy. It is well known that many molecules exhibit characteristic absorption lines in the THz region.[30] These spectra are generally very sharp, typically on the order of MHz when the concentration is at parts-per-million (ppm) levels, and also are distributed across a wide frequency range.[31,32] Thus, the ability of broadband and high-resolution detection of various gases is of particular importance in many applications such as quality assurance in industry, employee crisis management,[30] and breath analyses.[33] So far, infrared spectroscopy has been commonly used in gas spectroscopy,[34] but its detection range is in general very narrow and optimized for a specific gas. However, the number of important gases is increasing these days, and

15 July 2024 23:25:19

Published under an exclusive license by AIP Publishing

simultaneous detection of multiple gases distributed across a wide frequency region has been strongly desired.

In this study, gas-phase THz spectroscopy of acetonitrile (CH_3CN) was demonstrated. Acetonitrile is recognized as one of the most important nitrile compounds in astronomy,[35] atmospheric studies, and breath analysis.[36] Particularly, breath analysis of acetonitrile is considered for the diagnosis of lung cancer[37] or for testing drug abusers.[38] It has been well known that acetonitrile gas also exhibits rotational absorption lines in the THz region. This behavior can be theoretically explained by the Born–Oppenheimer approximation with a rigid rotor model.[39] According to this model, the rotational energy is given by $E_J = hBJ(J+1) + (A-B)K^2\hbar^2$, where J and K represent the quantum numbers quantized along the inertial axis and A and B are parameters related to the respective inertial moments. Accordingly, the absorption lines are expressed as $\nu = (E_{J+1} - E_J)/h = 2B(J+1)$ and are evenly spaced with $2B$, where the parameter B is 9.199 GHz for acetonitrile.[40] If the spectral resolution is sufficiently high, the fine structures $-2D_{JK}K^2(J+1)$ associated with the centrifugal distortion will be resolved in each J manifold. For acetonitrile, D_{JK} is known to be 177.4 kHz.

Frequency-domain THz spectra of acetonitrile gas in the range of 400–1100 GHz are depicted in Fig. 2(a). The vertical axis corresponds to the absorbance $\alpha = -(1/L_{\text{cell}})\log(I/I_0)$, where L_{cell} is the cell length and I/I_0 is the normalized transmission. A cylindrical gas cell with a length of $L_{\text{cell}} = 100$ mm and a diameter of $D = 18$ mm was used in this study. Both ends of the cell were sealed with Teflon plates, which are highly transparent in the THz range. A membrane-type pressure gauge was used to monitor the pressure inside the cell; the lowest detectable pressure was ~100 Pa. The gas cell was first evacuated down to ~1 Pa, and subsequently, acetonitrile gas was gradually introduced into the gas cell from the gas reservoir. The data were obtained every 10 MHz, and the gas pressure was 27 hPa. A series of absorption lines was clearly visible, and its averaged spacing was 18.3 GHz, in good agreement with the theoretically predicted values.

Figure 2(b) shows the absorbance data in the narrower range of 670–750 GHz. The frequency step was 10 MHz, and the gas pressure was 13 hPa. The numbers in the figure indicate the corresponding transitions, which are referenced to the database.[41] The data obtained by the previous technique are also shown for comparison. Similar behavior was confirmed in both measurements, but the data acquisition time differed significantly. Namely, the data acquisition rate of the previous technique was 720 points/h, and approximately 1.5 h was needed to cover the frequency span of 10 GHz. In contrast, the present technique was able to measure at a much higher rate, 66 000 points/h. Thus, it took only about 8 min to measure the data shown in the figure, corresponding to the scan speed of 180 MHz/s for every 10 MHz sampling.

Figure 3(a) shows the absorbance of dilute acetonitrile gas in the narrow range of 698.2–699.1 GHz. In this run, a few hPa of acetonitrile

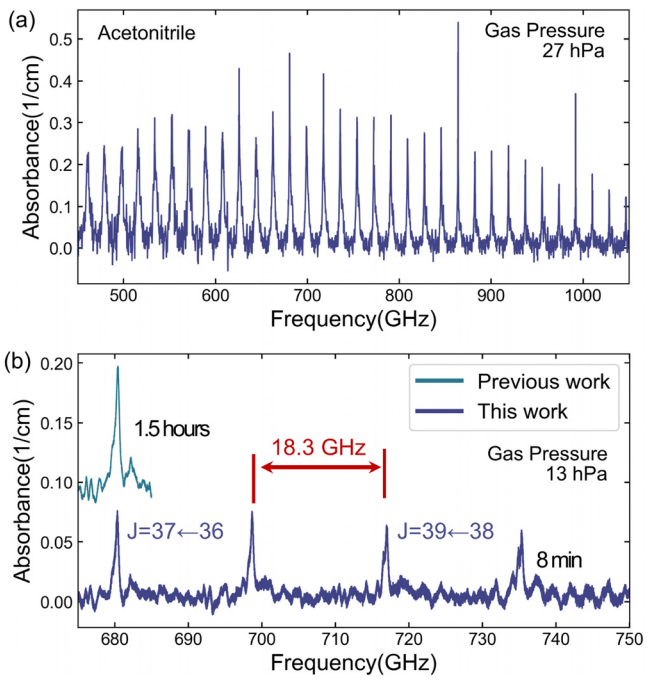

FIG. 2. Absorbance spectra of gas-phase acetonitrile (a) in the frequency range of 450–1100 GHz and (b) in the narrower range of 670–750 GHz. For comparison, the data taken by the previous technique (green line) are shown together, with a vertical offset for clarity.

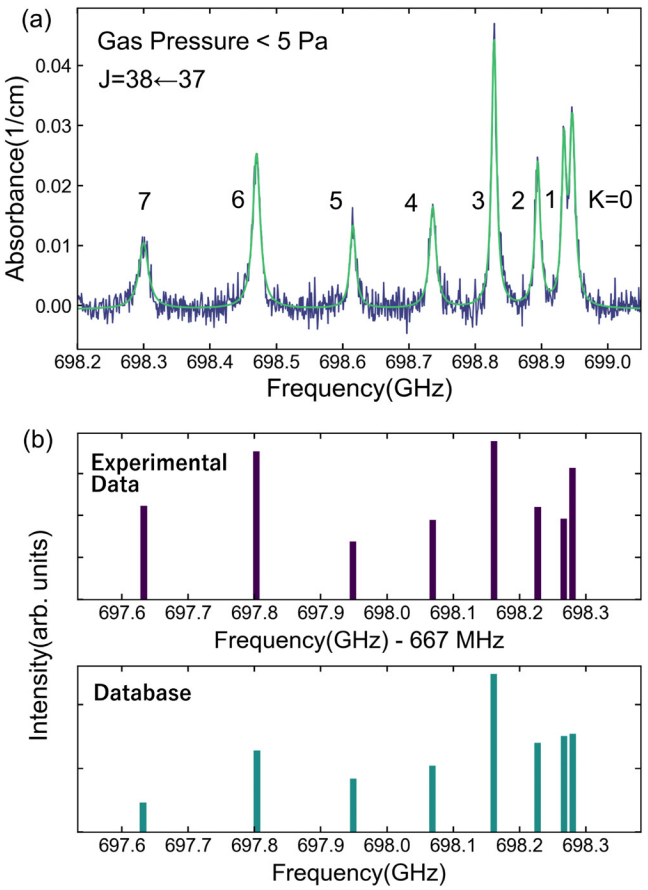

FIG. 3. (a) Fine structures of dilute acetonitrile gas observed in a narrow frequency range. The frequency step was 1 MHz. The result of multi-Lorentzian fitting is shown by the green curve. (b) Integrated intensity of each absorption line (upper frame) and those taken from the database (lower frame). The observe frequency values are uniformly offset by 666.9 MHz (see the text).

15 July 2024 23:25:19

Published under an exclusive license by AIP Publishing

gas was introduced to the cell and then evacuated with a rotary pump (150 L/min) for about 10 s. The pressure value was under the detection sensitivity of the absolute pressure gauge but estimated to be less than 5 Pa. A series of fine structures originating from the centrifugal distortion was clearly observed. The green line represents the result of multi-Lorentzian fitting. It should be noted that the observed full line widths at half maximum were typically between 8.1 and 17.4 MHz and that a small splitting of approximately 12.9 MHz near 699.0 GHz was clearly resolved.

As shown in Fig. 3(b), the integrated intensity of each spectrum was compared with those given in the database. The relative integrated intensity and the spacing showed good agreement with the database. It was found, however, that the observed frequencies were uniformly offset by 666.9 ± 0.6 MHz to the absolute frequency listed in the database. This result indicates that there are some errors in the frequency calibration, though they were within the accuracy of 2 GHz guaranteed by the supplier. This finding suggests that the absolute frequency of photomixing devices can be easily calibrated with an accuracy better than 1 MHz by this method across a wide frequency region.

Real-time gas spectroscopy of dilute acetonitrile gas is demonstrated in Fig. 4. A series of measurements was carried out while evacuating the gas cell. It took about 1 min to scan the frequency range between 698.2 and 699.1 GHz with a frequency step of ∼1 MHz. The slight temporal shifts in frequency were corrected. As the gas cell was being evacuated, the signal intensities gradually decreased, almost disappearing after 20 min, when the pressure was estimated to be around 1.5 Pa. The left inset shows the normalized absorbance spectra at 0, 2, and 4 min, together with the fitted Lorentzian curves. It is clearly seen that the linewidth monotonously decreased with time. The variation of the half width at the half maximum (HWHM) as a function of time is shown in the right inset. The observed behavior is consistent with the fact that collision-induced spectral broadening occurs as the pressure increases. It is noted that our apparatus clearly resolved slight changes in the spectral width on the order of 1 MHz.

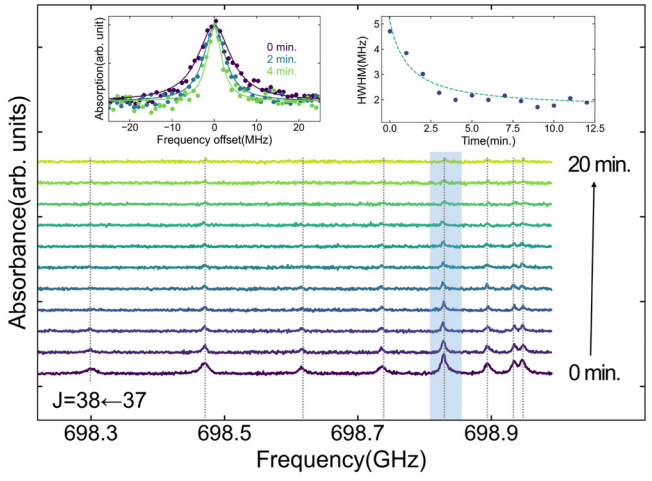

FIG. 4. Real-time gas-phase spectroscopy of dilute acetonitrile. The measurements were carried out during continuous evacuation for 20 min. The scan time of each trace was about 1 min. The hatched absorptions are analyzed in the left and right insets, which show the normalized absorbance spectra fitted with the Lorentzian curves and the variation of HWHF as a function of time, respectively.

As mentioned above, high-resolution frequency-domain THz spectrometers are important for detecting sharp resonances with linewidths of the order of 1–10 MHz. Characteristic specifications of these spectrometers are scan range, frequency accuracy/precision, scan speed, and sensitivity. For the case of photomixing devices, the scan range, which is determined by the detuning range of the source lasers, is typically beyond 1 THz and can be extended to 2.75 THz using an additional laser.[18] This seamless and wide scan range is one of most striking benefits of photomixing devices, compared to other solid-state-based[42] and vacuum-tube-based[43] oscillators. The frequency accuracy/precision somewhat depends on the source lasers but is sufficiently high in general: for instance, an accuracy of 1 GHz and a precision of 5 MHz are reported.[16]

Scan speed and sensitivity strongly depend on detection methods. Schottky diode detectors can measure the amplitude of THz waves directly, so the scan speed is only restricted either by the tuning speed or the detector bandwidth. On the other hand, homodyne detection takes more time to extract the frequency-dependent amplitude due to time-consuming phase scans,[21,25] though it is superior to Schottky detection in terms of sensitivity. Indeed, the SNR of the state-of-the-art preamplifier-integrated Schottky detector (bandwidth 1 MHz) was at best ∼50 dB for the source THz power of 1 μW.[44] This SNR value is less than that of homodyne detection, which can be better than 70 dB.

In this sense, homodyne-detection of frequency-domain THz spectroscopy has unique abilities of more sensitive detection, broadband frequency scan, and sufficiently high spectral resolution, but its bottle neck in applications has been the low data acquisition rate. The technique developed in this study improved the scan speed by almost two orders of our spectrometer, opening up promising opportunities for high-resolution and broadband THz spectroscopy. The limiting factor of the scan speed is currently a frequency bandwidth of the feedback circuit, which could be further increased by optimizing the circuit parameters in the future.

See the supplementary material for the comparison between the unlocked and locked photocurrents as a function of frequency.

This study was partly supported by a Grant-in-Aid for Scientific Research (B) (No. JP21H01040), the Nippon Sheet Glass Foundation for Materials Science and Engineering, and the CASIO Science Promotion Foundation.

AUTHOR DECLARATIONS

Conflict of Interest

The authors have no conflicts to disclose.

Author Contributions

Yuto Shoji: Conceptualization (equal); Formal analysis (lead); Investigation (lead); Methodology (equal); Writing – original draft (lead); Writing – review & editing (equal). **Eiji Ohmichi:** Conceptualization (equal); Formal analysis (equal); Funding acquisition (lead); Investigation (equal); Methodology (equal); Resources (equal); Supervision (lead); Writing – original draft (supporting); Writing – review & editing (equal). **Hideyuki Takahashi:** Formal analysis (supporting); Methodology (equal); Writing – original draft (supporting); Writing – review & editing (supporting). **Hitoshi Ohta:**

15 July 2024 23:25:19

Published under an exclusive license by AIP Publishing

Funding acquisition (supporting); Methodology (supporting); Resources (equal); Writing – original draft (supporting); Writing – review & editing (supporting).

DATA AVAILABILITY

The data that support the findings of this study are available from the corresponding author upon reasonable request.

REFERENCES

[1]M. Yahyapour, A. Jahn, K. Dutzi, T. Puppe, P. Leisching, B. Schmauss, N. Vieweg, and A. Deninger, "Fastest thickness measurements with a terahertz time-domain system based on electronically controlled optical sampling," Appl. Sci. **9**, 1283 (2019).

[2]I. S. Gregory, R. K. May, K. Su, and J. A. Zeitler, "Terahertz car paint thickness sensor: Out of the lab and into the factory," in *39th International Conference on Infrared, Millimeter, and Terahertz Waves (IRMMW-THz)* (IEEE, 2014).

[3]S. Brinkmann, N. Vieweg, G. Gärtner, P. Plew, and A. Deninger, "Towards quality control in pharmaceutical packaging: Screening folded boxes for package inserts," J. Infrared, Millimeter, Terahertz Waves **38**, 339–346 (2017).

[4]N. Rotenberg and L. Kuipers, "Mapping nanoscale light fields," Nat. Photonics **8**, 919–926 (2014).

[5]D. M. Mittleman, "Twenty years of terahertz imaging," Opt. Express **26**, 9417–9431 (2018).

[6]J. Neu and C. A. Schmuttenmaer, "Tutorial: An introduction to terahertz time domain spectroscopy (THz-TDS)," J. Appl. Phys. **124**, 231101 (2018).

[7]D. H. Auston, K. P. Cheung, and P. R. Smith, "Picosecond photoconducting hertzian dipoles," Appl. Phys. Lett. **45**, 284–286 (1984).

[8]P. U. Jepsen, D. G. Cooke, and M. Koch, "Terahertz spectroscopy and imaging–modern techniques and applications," Laser Photonics Rev. **5**, 124–166 (2011).

[9]S.-J. Kim, B. J. Kang, U. Puc, W. T. Kim, M. Jazbinsek, F. Rotermund, and O.-P. Kwon, "Highly nonlinear optical organic crystals for efficient terahertz wave generation, detection, and applications," Adv. Opt. Mater. **9**, 2101019 (2021).

[10]H. Hirori, A. Doi, F. Blanchard, and K. Tanaka, "Single-cycle terahertz pulses with amplitudes exceeding 1 MV/cm generated by optical rectification in $LiNbO_3$," Appl. Phys. Lett. **98**, 091106 (2011).

[11]R. B. Kohlhaas, S. Breuer, S. Nellen, L. Liebermeister, M. Schell, M. P. Semtsiv, W. T. Masselink, and B. Globisch, "Photoconductive terahertz detectors with 105 dB peak dynamic range made of rhodium doped InGaAs," Appl. Phys. Lett. **114**, 221103 (2019).

[12]N. Vieweg, F. Rettich, A. Deninger, H. Roehle, R. Dietz, T. Göbel, and M. Schell, "Terahertz-time domain spectrometer with 90 dB peak dynamic range," J. Infrared, Millimeter, Terahertz Waves **35**, 823–832 (2014).

[13]U. Nandi, J. Norman, A. Gossard, H. Lu, and S. Preu, "1550-nm driven ErAs: In (Al) GaAs photoconductor-based terahertz time domain system with 6.5 THz bandwidth," J. Infrared, Millimeter, Terahertz Waves **39**, 340–348 (2018).

[14]S. Verghese, K. McIntosh, S. Calawa, W. Dinatale, E. Duerr, and K. Molvar, "Generation and detection of coherent terahertz waves using two photomixers," Appl. Phys. Lett. **73**, 3824–3826 (1998).

[15]S. Preu, G. Döhler, S. Malzer, L. Wang, and A. Gossard, "Tunable, continuous-wave terahertz photomixer sources and applications," J. Appl. Phys. **109**, 061301 (2011).

[16]D. Stanze, A. Deninger, A. Roggenbuck, S. Schindler, M. Schlak, and B. Sartorius, "Compact cw terahertz spectrometer pumped at 1.5 μm wavelength," J. Infrared, Millimeter, Terahertz Waves **32**, 225–232 (2011).

[17]T. Göbel, D. Stanze, B. Globisch, R. J. Dietz, H. Roehle, and M. Schell, "Telecom technology based continuous wave terahertz photomixing system with 105 decibel signal-to-noise ratio and 3.5 terahertz bandwidth," Opt. Lett. **38**, 4197–4199 (2013).

[18]A. J. Deninger, A. Roggenbuck, S. Schindler, and S. Preu, "2.75 THz tuning with a triple-DFB laser system at 1550 nm and InGaAs photomixers," J. Infrared, Millimeter, Terahertz Waves **36**, 269–277 (2015).

[19]L. Liebermeister, S. Nellen, R. Kohlhaas, S. Breuer, M. Schell, and B. Globisch, "Ultra-fast, high-bandwidth coherent cw THz spectrometer for non-destructive testing," J. Infrared, Millimeter, Terahertz Waves **40**, 288–296 (2019).

[20]M. Deumer, S. Breuer, R. Kohlhaas, S. Nellen, L. Liebermeister, S. Lauck, M. Schell, and B. Globisch, "Continuous wave terahertz receivers with 4.5 THz bandwidth and 112 dB dynamic range," Opt. Express **29**, 41819–41826 (2021).

[21]E. Ohmichi, Y. Shoji, H. Takahashi, and H. Ohta, "Frequency-domain electron spin resonance spectroscopy using continuously frequency-tunable terahertz photomixers," Appl. Phys. Lett. **119**, 162404 (2021).

[22]D. W. Vogt and R. Leonhardt, "High resolution terahertz spectroscopy of a whispering gallery mode bubble resonator using Hilbert analysis," Opt. Express **25**, 16860–16866 (2017).

[23]E. Ohmichi, T. Fujimoto, K. Minato, and H. Ohta, "Terahertz electron paramagnetic resonance spectroscopy using continuous-wave frequency-tunable photomixers based on photoconductive antennae," Appl. Phys. Lett. **116**, 051101 (2020).

[24]E. Ohmichi, Y. Shoji, H. Takahashi, and H. Ohta, "Frequency-domain antiferromagnetic resonance spectroscopy of NiO," J. Phys. Soc. Jpn. **91**, 095001 (2022).

[25]Y. Shoji, E. Ohmichi, H. Takahashi, and H. Ohta, "High-resolution frequency-domain terahertz spectroscopy and its application to electron paramagnetic resonance," in *46th International Conference on Infrared, Millimeter and Terahertz Waves (IRMMW-THz)* (IEEE, 2021).

[26]A. Roggenbuck, K. Thirunavukkuarasu, H. Schmitz, J. Marx, A. Deninger, I. C. Mayorga, R. Güsten, J. Hemberger, and M. Grüninger, "Using a fiber stretcher as a fast phase modulator in a continuous wave terahertz spectrometer," J. Opt. Soc. Am. B **29**, 614–620 (2012).

[27]E. Brown, F. Smith, and K. McIntosh, "Coherent millimeter-wave generation by heterodyne conversion in low-temperature-grown GaAs photoconductors," J. Appl. Phys. **73**, 1480–1484 (1993).

[28]A. Roggenbuck, H. Schmitz, A. Deninger, I. C. Mayorga, J. Hemberger, R. Güsten, and M. Grüninger, "Coherent broadband continuous-wave terahertz spectroscopy on solid-state samples," New J. Phys. **12**, 043017 (2010).

[29]D.-Y. Kong, X.-J. Wu, B. Wang, Y. Gao, J. Dai, L. Wang, C.-J. Ruan, and J.-G. Miao, "High resolution continuous wave terahertz spectroscopy on solid-state samples with coherent detection," Opt. Express **26**, 17964–17976 (2018).

[30]L. Yang, T. Guo, X. Zhang, S. Cao, and X. Ding, "Toxic chemical compound detection by terahertz spectroscopy: A review," Rev. Anal. Chem. **37**, 20170021 (2018).

[31]G.-R. Kim, H.-B. Lee, and T.-I. Jeon, "Terahertz time-domain spectroscopy of low-concentration N_2O using long-range multipass gas cell," IEEE Trans. Terahertz Sci. Technol. **10**, 524–530 (2020).

[32]Y.-D. Hsieh, H. Kimura, K. Hayashi, T. Minamikawa, Y. Mizutani, H. Yamamoto, T. Iwata, H. Inaba, K. Minoshima, F. Hindle *et al.*, "Terahertz frequency-domain spectroscopy of low-pressure acetonitrile gas by a photomixing terahertz synthesizer referenced to dual optical frequency combs," J. Infrared, Millimeter, Terahertz Waves **37**, 903–915 (2016).

[33]N. Rothbart, O. Holz, R. Koczulla, K. Schmalz, and H.-W. Hübers, "Analysis of human breath by millimeter-wave/terahertz spectroscopy," Sensors **19**, 2719 (2019).

[34]B. Stuart, "Infrared spectroscopy," in *Kirk-Othmer Encyclopedia of Chemical Technology* (John Wiley & Sons, Inc., 2000).

[35]A. J. Remijan, J. M. Hollis, F. J. Lovas, D. F. Plusquellic, and P. Jewell, "Interstellar isomers: The importance of bonding energy differences," Astrophys. J. **632**, 333 (2005).

[36]M. Li, J. Ding, H. Gu, Y. Zhang, S. Pan, N. Xu, H. Chen, and H. Li, "Facilitated diffusion of acetonitrile revealed by quantitative breath analysis using extractive electrospray ionization mass spectrometry," Sci. Rep. **3**, 1205 (2013).

[37]J. K. Campbell, J. W. Rhoades, and A. L. Gross, "Acetonitrile as a constituent of cigarette smoke," Nature **198**, 991–992 (1963).

[38]S. Giacomuzzi, Y. Riemer, M. Pavlic, A. Schmid, H. Hinterhuber, and A. Amann, "Applications of breath gas analysis in addiction medicine–preliminary results," Subst. UseMisuse **44**, 301–304 (2009).

[39]M. Born and R. Oppenheimer, "Zur quantentheorie der molekeln," Ann. Phys. **389**, 457–484 (1927).

[40]J. Pearson and H. Müller, "The submillimeter wave spectrum of isotopic methyl cyanide," Astrophys. J. **471**, 1067 (1996).

15 July 2024 23:25:19

Published under an exclusive license by AIP Publishing

[41]H. Pickett, R. Poynter, E. Cohen, M. Delitsky, J. Pearson, and H. Müller, "Submillimeter, millimeter, and microwave spectral line catalog," J. Quant. Spectrosc. Radiat. Transfer **60**, 883–890 (1998).
[42]W. Kou, S. Liang, H. Zhou, Y. Dong, S. Gong, Z. Yang, and H. Zeng, "A review of terahertz sources based on planar Schottky diodes," Chin. J. Electron. **31**, 467–487 (2022).
[43]C. Paoloni, D. Gamzina, R. Letizia, Y. Zheng, and N. C. Luhmann, Jr., "Millimeter wave traveling wave tubes for the 21st century," J. Electromagn. Waves Appl. **35**, 567–603 (2021).
[44]M. Yahyapour, N. Vieweg, A. Roggenbuck, F. Rettich, O. Cojocari, and A. Deninger, "A flexible phase-insensitive system for broadband cw-terahertz spectroscopy and imaging," IEEE Trans. Terahertz Sci. Technol. **6**, 670–673 (2016).

15 July 2024 23:25:19

Published under an exclusive license by AIP Publishing